

CHAPTER 8. Thermal Studies.

1. Introduction.

IR quadrupoles will work in a hard radiation environment that produces a high level of heat deposition in the coil [1]. Thermal analysis has been performed during a conceptual design study to optimize the magnet design and to prove its workability in LHC. The magnet workability was described in term of an operational margin defined as follows:

$$\text{operational margin} = \Delta T_c : \Delta T_{cbl},$$

where

$\Delta T_c = T_c - T_b$ – cable critical temperature margin,

$\Delta T_{cbl} = T_{cbl} - T_b$ – turn temperature rise,

T_c and T_{cbl} – cable critical and operation temperatures,

T_b – HeII temperature.

The results of calculations of the temperature rise in the inner and outer layer mid-plane turns exposed to the maximum radiation heating power, and the operational margin of the inner and outer layers at nominal field gradient of 205 T/m are reported in Table 1. Calculations were performed for nominal LHC luminosity for two cases of coil cooling conditions (see details in TDH [2]).

Table 1. Temperature rise of the inner and outer midplane turns and operational margin of the inner and outer layer at different coil cooling conditions and $G=205$ T/m.

Cooling Cond.	Pmax, mW/g	Pin, W/m	Pout, W/m	Inner layer,		Outer layer,	
				ΔT_{cbl} , K	$\Delta T_c : \Delta T_{cbl}$	ΔT_{cbl} , K	$\Delta T_c : \Delta T_{cbl}$
nominal	0.55	0.08	0.026	0.11	21.8	1.3	2.85
poor	0.6	0.087	0.028	1.09	2.17	2.8	1.32

The temperature margin at the nominal field gradient of 205 T/m for the inner-layer midplane turns is $\Delta T_c = 2.4$ K, and for the outer-layer midplane turns - $\Delta T_c = 3.7$ K. The nominal cooling conditions corresponded to the case of presence of the inter-turn cooling channels in the magnet inner layer, and poor cooling conditions corresponds to the case when these channels do not work (are closed) for some reason. Based on these data it was concluded that the developed magnet design provides a sufficient operational margin under expected LHC operational conditions.

During the short model R&D phase an experimental verification of HGQ thermal model were performed using special short model with high level of AC losses in the coil. Based on the obtained results and results of recent calculations of the radiation heat deposition distribution in the IR inner triplets new calculations of magnet operation

margin have been performed using FEA thermal model. The results of these works are reported in this chapter.

2. Thermal model experimental verification.

The idea of experimental verification of the HGQ thermal calculations is based on measurements of sensitivity of magnet critical current to the AC loss heat depositions in the coil.

Three models HGQ06, 07 and 08 demonstrated a high level of AC losses in the coil comparable with the level of radiation heat depositions (see Figure 1.).

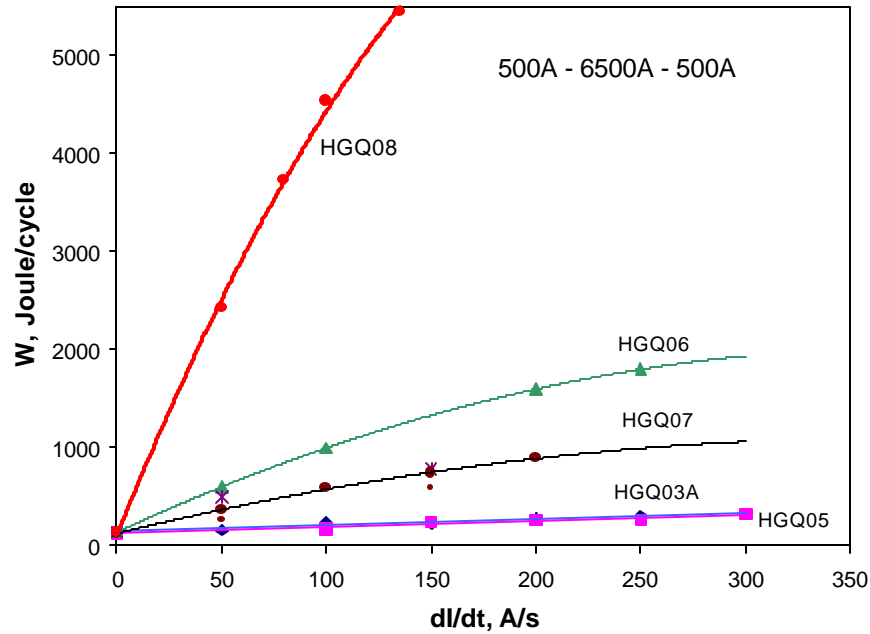


Figure 1. AC losses in the triangular cycle with current amplitude change within 500-6500 A range vs the current ramp rate.

However, for the purpose of this study a uniformity of the cable interstrand resistance was very important. The data presented in Table 2 show that the best uniformity of interstrand resistance represented by the eddy current components in low order field harmonics was achieved in HGQ08 made of stabrite cable. The data obtained for this model was used for further thermal analysis.

Table 2. Eddy current field components and AC losses measured in HGQ05-08.

Model number	Eddy current field component @ dI/dt=80 A/s, 10 ⁻⁴						W(100A/s), J/cycle
	b6	b10	b3	a3	b4	a4	
HGQ05	<0.02	<0.02	<0.2	<0.1	0	<0.1	177.4
HGQ06	+3.7	-0.1	-13	-8	-3	0	1000
HGQ07	+1.1	-0.1	+31	+32	-1	+18	589
HGQ08	+0.8	-0.6	+8	+10	-1	+2	4538

The results of measurement of ramp rate dependence of magnet quench current vs current ramp rate for HGQ08 at different HeII temperatures are presented in Figure 2. It was found that high ramp rate quenches were originated in the turns close to the coil midplanes.

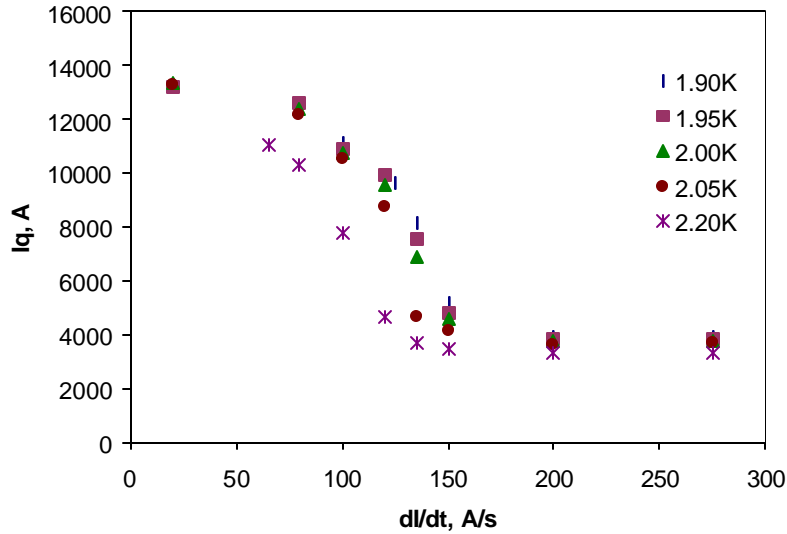


Figure 2. Quench current vs current ramp rate measured at different helium temperature.

To transform the ramp rate numbers on the horizontal axis of the plot in Figure 2 into the corresponding heating power in the quenched midplane turns the results of AC loss measurements in the magnet were used. The AC loss power in the HGQ08 coil as function of current ramp rate is shown in Figure 3.

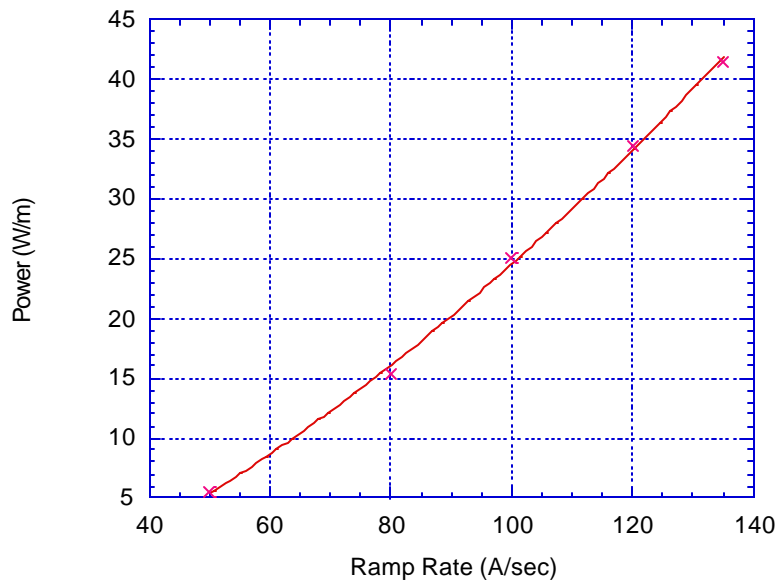


Figure 3. AC loss power in HGQ08 coil vs current ramp rate.

Each point in the above plot was determined as follows. At each ramp rate, the five measurements of energy lost for a ramp from 500 A to 6500 A and back to 500 A were averaged to give a net energy into the magnet. Similarly, the five measurements at each ramp rate for a ramp to 4000 A and to 3500 A were averaged to give net energy into the magnet. Then, for each ramp rate, the energy at 4000 A was subtracted from the energy at 6500 A and divided by the time difference for the two cycles. This subtracts out the end effects (ramp acceleration and deceleration) and gives a power for just the fixed ramp rate. Dividing by the 1.8 m magnet length gives W/m. The same subtraction and power calculation was done for the 6500 A and 3500 A data. Then the two points at each ramp rate (6500 minus 3500 results and 6500 minus 4000 results) were averaged to give the points which are plotted above. The curve is a quadratic fit that is not forced to go through zero.

To determine the AC loss power generated in the midplane turns based on the measured total AC loss power in the coil the theoretical distribution of AC losses in the HGQ08 coil was used. This distribution and the expected distribution of radiation heat depositions in the coil are shown in Figure 4.

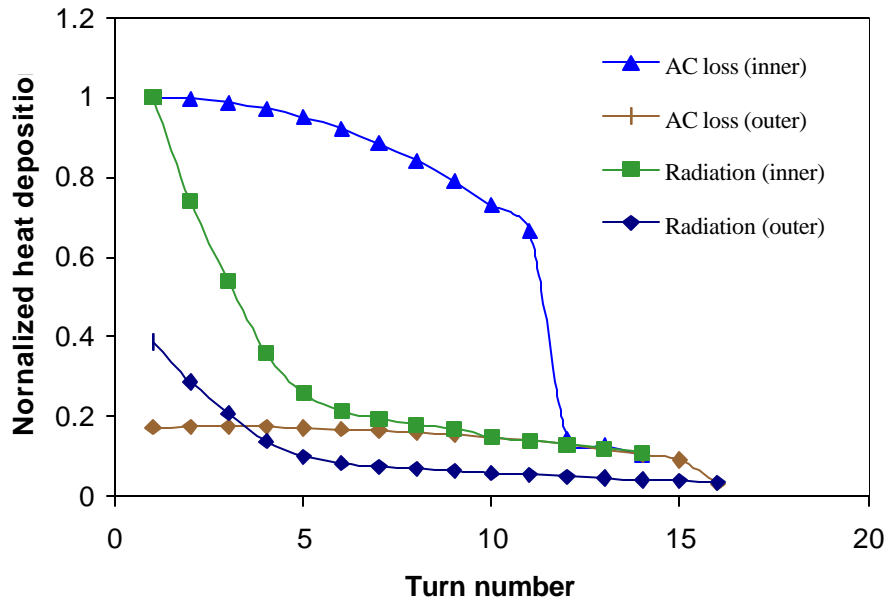


Figure 4. Distribution of AC Losses and radiation heat deposition in the HGQ coil ($dI/dt=100$ A/s)

Heat depositions are normalized to that at the midplane in the inner coil. Note that the heat generated by the AC losses is more uniformly distributed over the inner and outer layers than what is expected for radiation heating in LHC. Thus, in LHC a smaller by factor of 2.2 total coil heat load will have the same impact on the coil at the midplane.

Based on the above distribution the AC loss power in each midplane turn is about 1% of the total AC loss power in the coil. The dependence of AC loss power in midplane turns vs current ramp rate for HGQ08 is summarized in Table 3. As it can be seen the level of radiation heat deposition presented in Table 1 is reached at current ramp rate of ~ 60 A/s.

Table 3. Measured AC loss power in the HGQ08 coil and calculated total AC loss power and AC loss power in the midplane turns at different current ramp rates.

dI/dt, A/s	Pmeas, W/m	Pcalc, W/m	Ra, 10^{-9} Ohm*m	Ra, mcOhm	Pin1/Ptot	Pin1, W/m
50	5.82	5.8	5.3	1.46	0.01	0.0582
60	8.16	8.15	5.4	1.49	0.01	0.0816
70	10.83	10.84	5.5	1.52	0.01	0.1083
80	13.8	13.87	5.6	1.54	0.01	0.1380

Finally based on the above experimental results and theoretical analysis for the quenches originated in the midplane turns the dependence of turn quench current vs the power generated in the turn for different HeII temperature was obtained. The plot is shown in Figure 5. As it follows from the above plot, the steady state power required to quench midplane turn at the current corresponding to the nominal field gradient of 205 T/m is $P_{max} \sim 0.18$ W/m at HeII temperatures of 1.9-2.05 K. At He temperature above lambda-point the cable cooling conditions are drastically deteriorated and quench power is reduced by factor of 2.

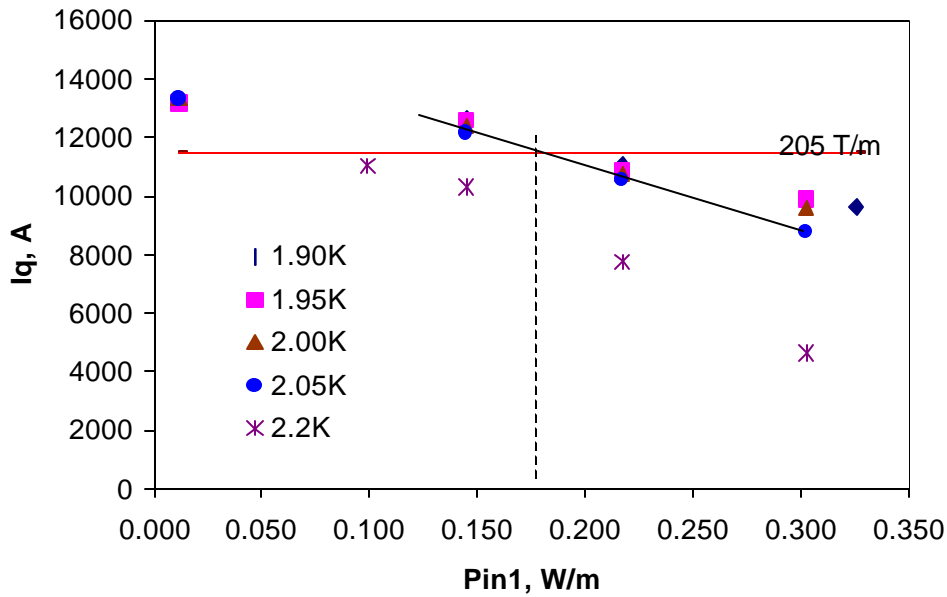


Figure 5. Dependence of the midplane turn quench current vs the heating power.

Based on the above data, the operational margin of the inner-layer midplane turns could be defined as

$$\text{operational margin} = \Delta T_c : \Delta T_{cbl} = P_{max} / P_{rad},$$

and is $0.18/0.08=2.25$. This number is in a good agreement with 2.17 reported in Table 1 for the inner layer for the case of poor cooling conditions when inter-turn cooling channels in the inner layer do not work.

The good agreement of the measurements with calculated margin for the inner layer gives a confidence in the prediction for the outer cable, which is what will limit magnet performance.

3. Thermal model update.

a. Magnet coil

Experimental studies described in previous section provided the information concerning the real coil cooling conditions in the coil and conformed the magnet operational margin determined using a simple analytical model. To improve and update the HGQ thermal analysis a 2-D ANSYS® steady thermal model has been created. The model is based on the octant symmetry (see Figure 6) and includes inner and outer coils, ground insulation, and stainless steel collars.

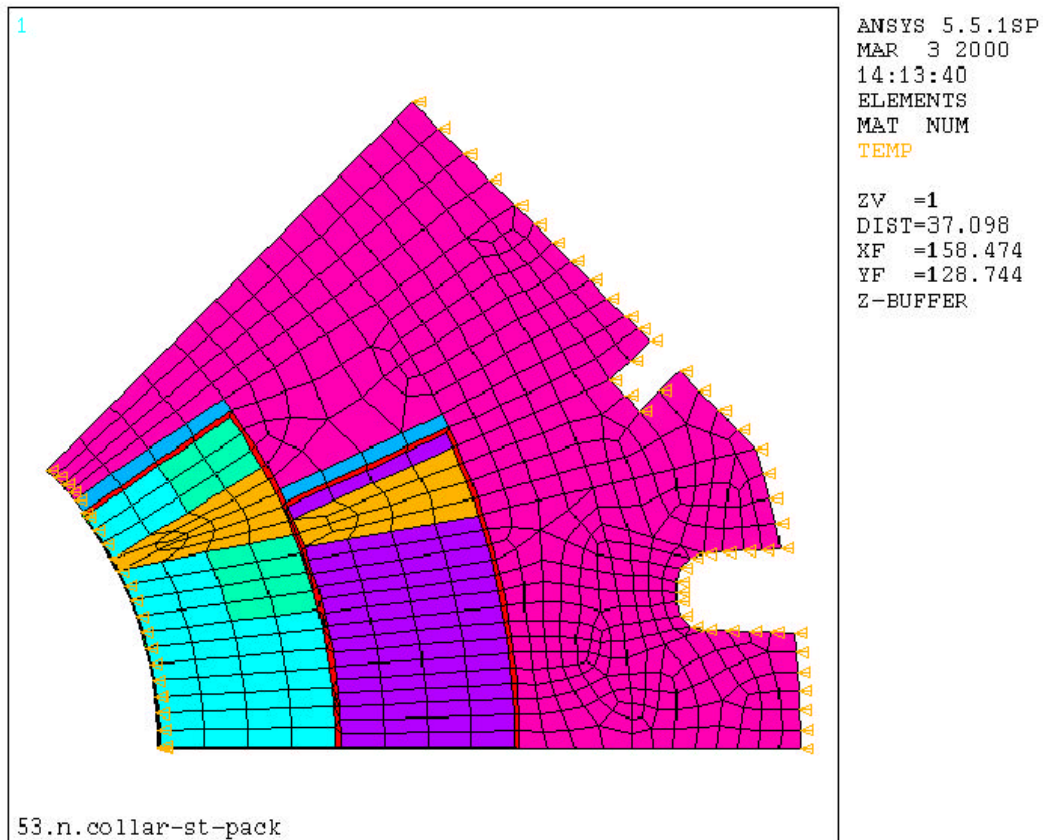


Figure 6. ANSYS thermal model of the HGQ collared coil.

Thermal conductivity for the collared coil elements at 2 K are presented below:

Kapton (ground and cable insulation) – $\lambda = 0.005 \text{ W/m}^*\text{K}$

Stainless Steel (collar) – $\lambda = 0.1 \text{ W/m}^*\text{K}$

Copper (strand matrix) – $\lambda = 140 \text{ W/m}^*\text{K}$

Inner/outer coil azimuthal – $\lambda = 2.0 \text{ W/m}^*\text{K}$

Inner coil radial – $\lambda = 19.8 \text{ W/m}^*\text{K}$

Outer coil radial – $\lambda = 22.0 \text{ W/m}^*\text{K}$

Kapitza resistance on the Kapton-HeII interface was simulated by the layer with a thickness δ (measured in meters) and a thermal conductivity $\lambda = 300 * \delta$ W/m*K.

Boundary conditions include constant temperature of HeII of 1.9 K in the annular channel and on the outer surface of the coil, and zero heat flux through the midplane.

The calculated temperature distribution in the coil for the nominal radiation heat depositions [Mokhov, March 2000] is shown in Figure 7.

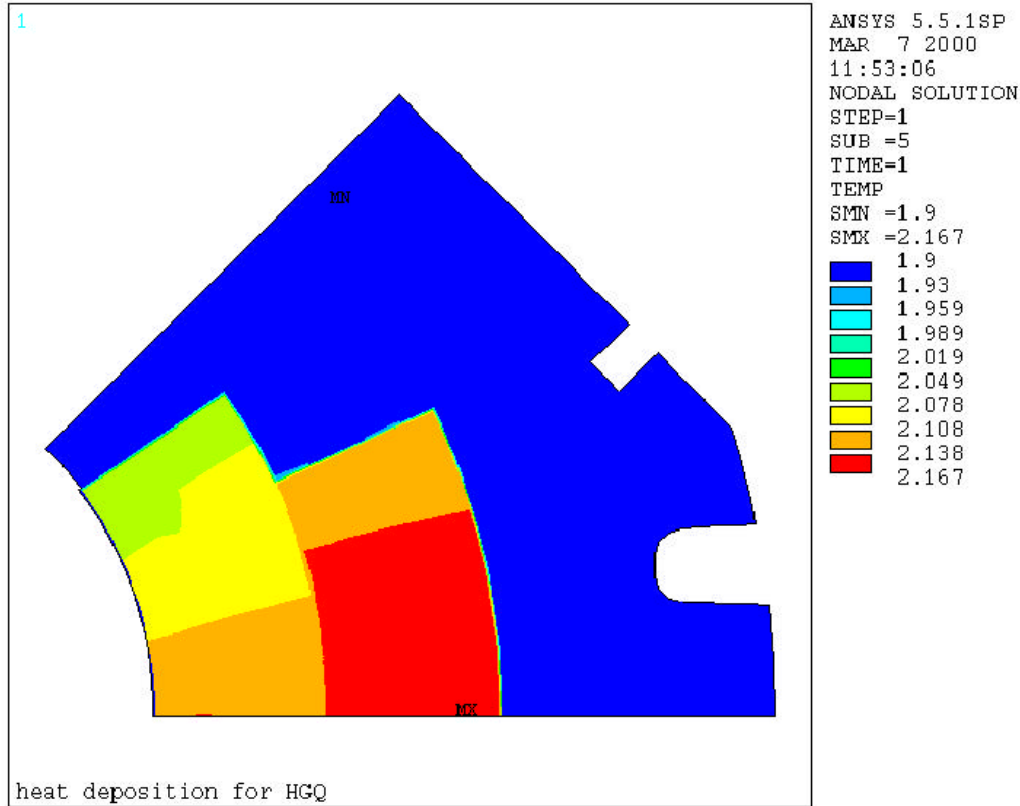


Figure 7. Temperature distribution in the HGQ coil at nominal LHC radiation heat deposition.

The results of calculations show that radial and azimuthal temperature gradients in each layer are small in spite of the strong radial and azimuthal dependence of radiation heat deposition in the coil. The temperature in the inner layer changes from maximum value of 2.134 K in the midplane turn to 2.072 K in the pole turn. The temperature in the outer layer changes from 2.167 K in the midplane to 2.134 K in pole region. Radial gradient in both layers less than 5 K.

Distributions of radiation heat deposition and cable/turn temperature in the HGQ coil inner and outer layers at nominal LHC luminosity, and turn temperature margin at 205 T/m field gradient are shown in Figure 8. The results of calculation of turn operation margin for nominal luminosity are reported in Figure 9.

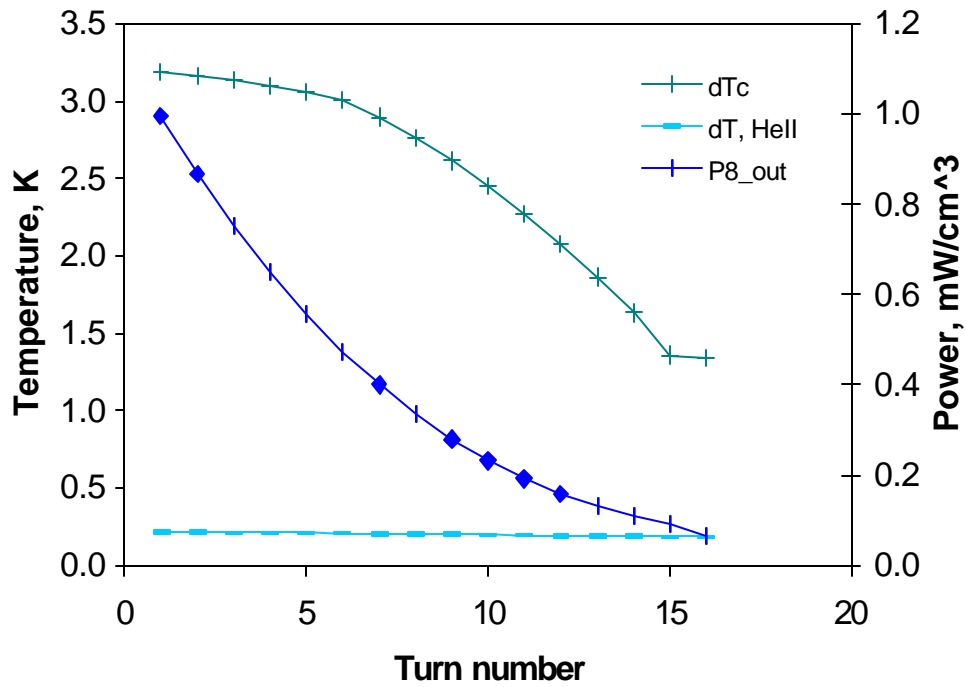
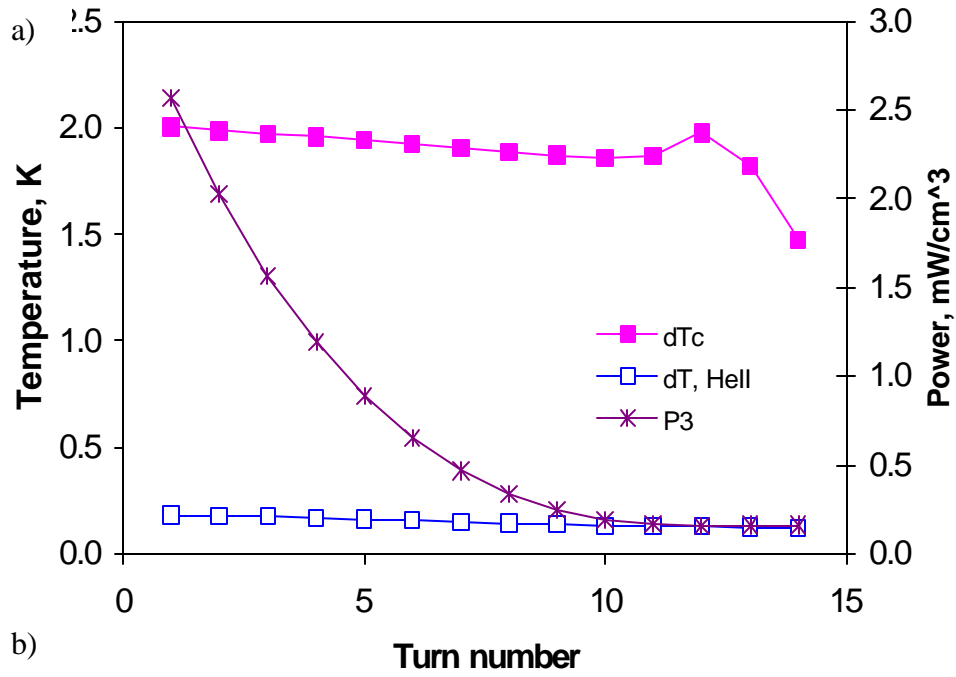


Figure 8. Distribution of radiation heat deposition and temperature, and temperature temperature margin in the HGQ coil: a) inner layer; b) outer layer.

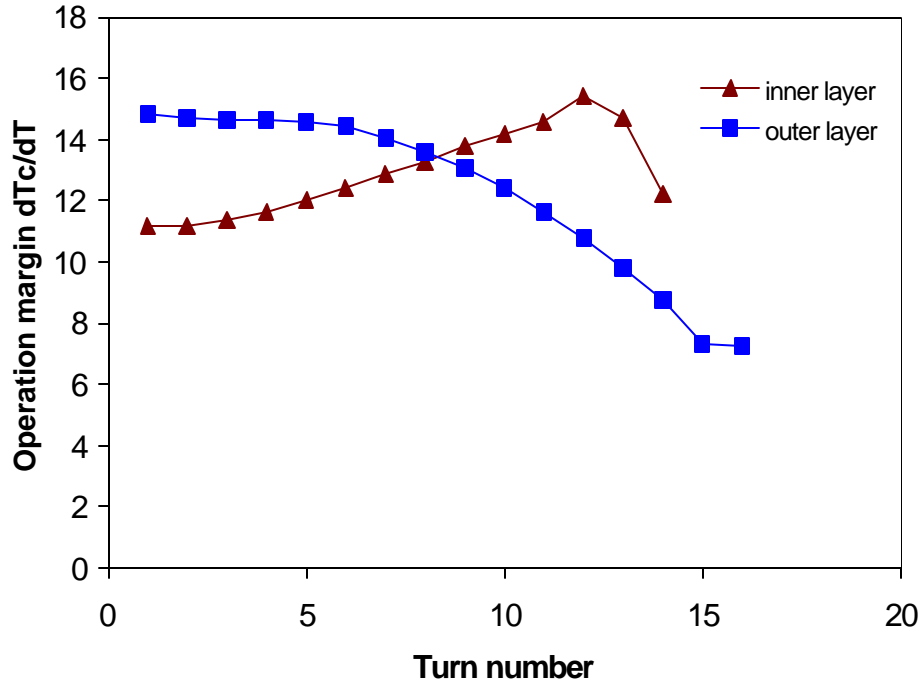


Figure 9. Operational margin for inner and outer turns at nominal field gradient of 205 T/m.

As it can be seen the operational margin of inner layer is ~ 11 and determined by the midplane turns. Operational margin of outer layer is ~ 7 and determined by the pole turns. Thus, the outer layer determines the magnet operational margin that is ~ 7 for the nominal LHC luminosity. This margin is also sufficient to provide the reliable magnet operation at expected ultimate luminosity which is by factor of 2.5 higher.

b. Heat transfer inside magnet

One important region of heat transfer not included in the above analysis is from the bore tube region out to the holes in the iron yoke. This heat transfer must occur through the pole tip region between the coils. Assume the heat all starts in the bore tube region. The heat will be smoothly distributed circumferentially by the 1 mm gap between the coil and bore tube, so the four quadrants share the radial heat flow equally.

Radial heat flow is out gaps in the pole tips created by periodically leaving out pole tip spacers, the thickness of one lamination. Since the temperature difference increases with heat flux cubed, the ΔT increases with pole tip open fraction cubed. Thus, ΔT is very sensitive to heat flux and gap spacing. ΔT 's of 5 mK become significant in the total picture; 5 mK is about 5% of the estimated temperature rise through the whole inner triplet with ultimate luminosity. Thus, we should design the collar region for heat transfer with no more than 5 mK, preferably only a few mK.

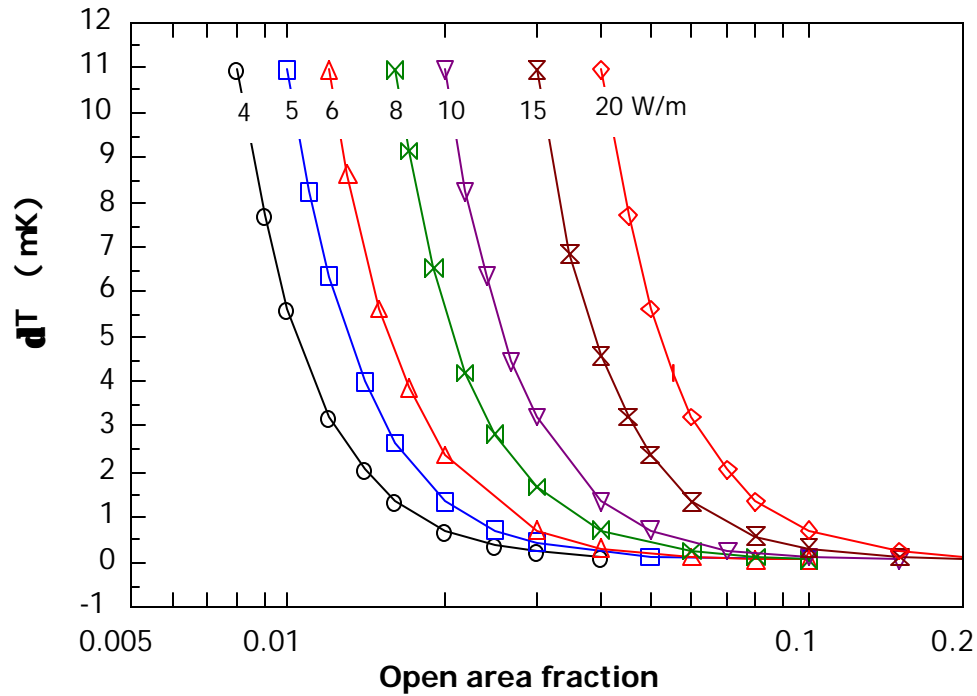


Figure 10. Delta-T through the collar pole tip region versus fraction of pole tip area open for heat transport

For the Fermilab quad a 0.7 cm wide pole tip, a 1.6 cm distance for heat transfer radially outward, and a missing lamination provides a 1.52 mm thick gap. Thus, the heat flow area per missing tip is 0.106 cm. In order to have only a 5 mK temperature rise through the collars in Q2, where the local heat load could be 15 W/m, one can see from Figure 10 that the pole tip area must be 0.04 open. A fraction of 0.04 open implies gaps equivalent to a missing collar lamination every 1.5 inches in each quadrant.

At CERN in March, 1998, a requirement for the total cross-sectional area of free flow passages the equivalent of four 45 mm holes, or 63.6 sq cm flow area, through the iron yoke was chosen. This requirement was based on superfluid heat transport properties and the anticipated nominal heat loads plus a 25% margin. The cooldown and quench flow area requirement is less severe. Eight 32 mm holes would provide the same area and result in the same temperature profiles as four 45 mm holes. For comparison, the LHC dipole cold mass hydraulic passage requirement is the equivalent of one 50 mm inner diameter tube [LHC Project Note 135].

However, heat removal with ultimate luminosity requires larger yoke holes than the March, 1998 criterion. Fortunately, KEK retained the 60 mm yoke holes (for Q1 and Q3) and Fermilab 50 mm yoke holes (for Q2). The result in each case is about a 14 mK delta-T with ultimate luminosity, as can be seen in Figure 11 below.

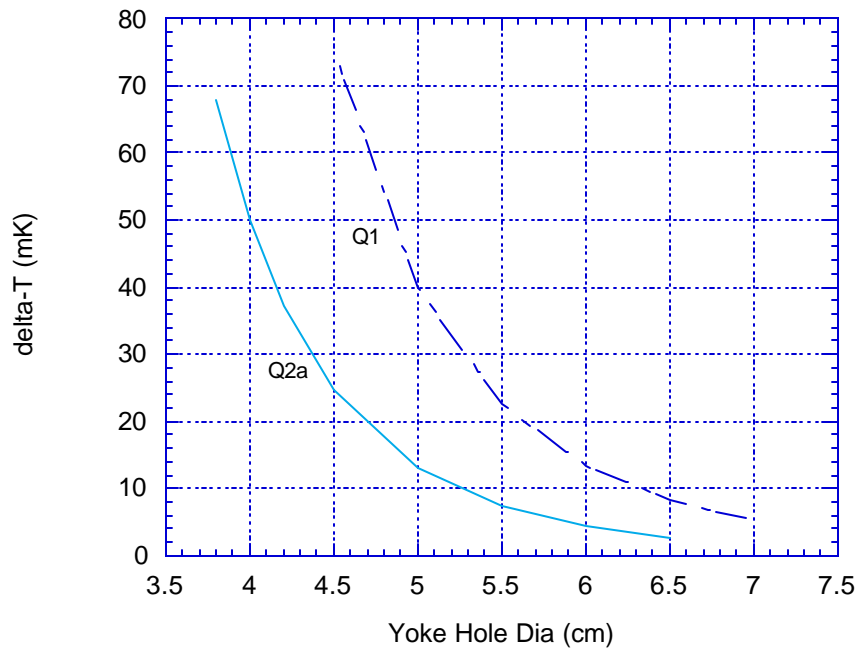


Figure 11. A plot of delta-T axially through the yoke holes in Q1 and Q2a versus hole size assuming four holes and the ultimate heat load.

4. Summary.

The results reported in this chapter could be summarized as follows:

- ◆ Thermal study shows that coil cooling conditions corresponds to the case when channels in the inner-layer insulation are closed and thus do not work. This will be visually checked in mechanical model.
- ◆ Measurement results show that the heat flux density from the coil (at coil surface) is well below its critical value.
- ◆ For the heat deposition in the midplane inner-coil turns of 0.08 W/m measured operation margin for inner layer is 2.25 that is in a good agreement with calculated value of 2.17. It does not change significantly with helium temperature because it is determined mainly by the insulation thermal resistance.
- ◆ For nominal LHC luminosity magnet temperature margin is determined by the outer layer margin that is ~7.
- ◆ This magnet design does have enough margin to work at the expected ultimate luminosity too.

REFERENCES.

- 1.
- 2.
- 3.